



HAL
open science

Positive Cooperative Effect in Ion-Pair Recognition by a Tris-urea Hemicryptophane Cage

Magalie Delecluse, Cédric Colombar, Delphine Moraleda, Innocenzo de Riggi, Françoise Duprat, Sabine Michaud-Chevallier, Jean-Pierre Dutasta, Vincent Robert, Bastien Chatelet, Alexandre Martinez

► **To cite this version:**

Magalie Delecluse, Cédric Colombar, Delphine Moraleda, Innocenzo de Riggi, Françoise Duprat, et al.. Positive Cooperative Effect in Ion-Pair Recognition by a Tris-urea Hemicryptophane Cage. Chemistry - A European Journal, Wiley-VCH Verlag, 2019, 25 (13), pp.3337-3342. 10.1002/chem.201805534 . hal-02098293

HAL Id: hal-02098293

<https://hal.archives-ouvertes.fr/hal-02098293>

Submitted on 23 Mar 2020

HAL is a multi-disciplinary open access archive for the deposit and dissemination of scientific research documents, whether they are published or not. The documents may come from teaching and research institutions in France or abroad, or from public or private research centers.

L'archive ouverte pluridisciplinaire **HAL**, est destinée au dépôt et à la diffusion de documents scientifiques de niveau recherche, publiés ou non, émanant des établissements d'enseignement et de recherche français ou étrangers, des laboratoires publics ou privés.

Positive Cooperative Effect in Ion-Pair Recognition by a Tris-urea Hemicyptophane Cage

Delecluse, M., Colombar, C., Moraleda, D., de Riggi, I., Duprat, F., Michaud-Chevallier, S., Dutasta, J. P., Robert, V., Chatelet, B., Martinez, A.

Abstract: The synthesis of a hemicyptophane cage combining a CTV unit with a C_3 symmetrical moiety bearing three urea functions is reported. This host was found to bind anions with higher binding constants than other previously reported hemicyptophanes. Due to its heteroditopic charac-

ter this cage proved to be an efficient ion-pair receptor. The best cooperativity effect was observed for the tetramethylammonium bromide (TMABr) salt, which was confirmed and rationalized by DFT calculations.

Introduction

The design of receptors capable of simultaneously binding cations and anions have recently attracted a growing attention.^[1–12] The so-called heteroditopic ion-pair receptors indeed displays remarkably improved binding affinities and selectivities compared to related single ion receptors. It has been proposed that the positive cooperativity effect observed in these systems arise from attractive electrostatic interactions between the two co-bound ions. This emergent class of hosts have found numerous applications ranging from salt solubilization, ion sensing, ion extraction and transport of ion pairs through membranes.^[13] Among the various host molecules designed to bind salts inside their cavity, hemicyptophanes have recently emerged as a new class of receptors capable of recognizing ion pairs. Contrary to the homotopic cryptophanes receptors,^[14] the cavity of hemicyptophanes is heteroditopic in nature as it is build from a cyclotrimeratrylene (CTV) unit (upper part), connected to another different C_3 symmetrical moiety (lower part).^[15] In particular, the ability of the hemicyptophane **1** to complex tetramethylammonium halide (TMA-halide) salts

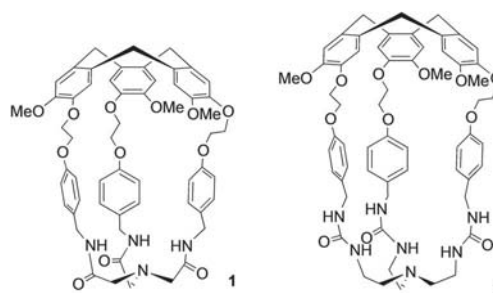
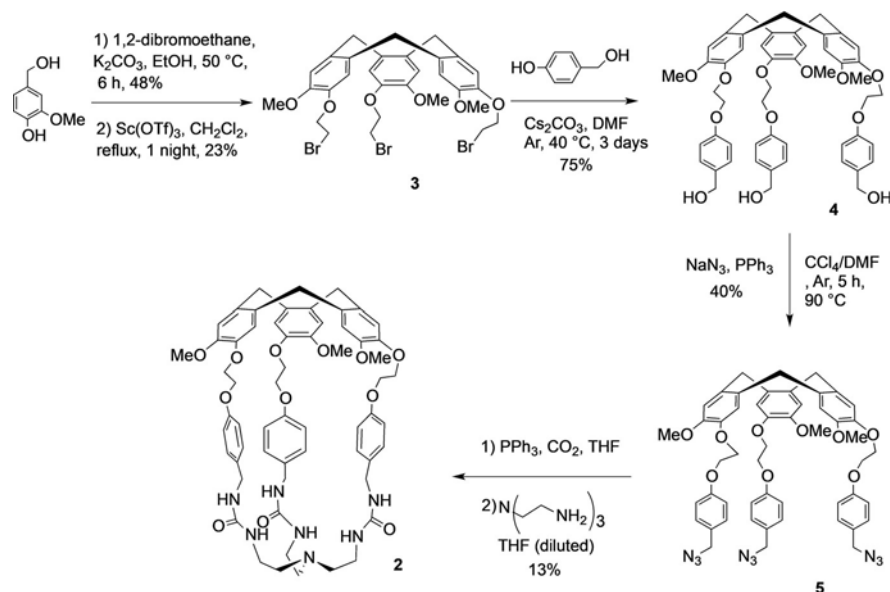


Figure 1. Structures of hemicyptophanes **1** and **2**.

with a positive cooperativity has been demonstrated (Figure 1).^[16] It was shown that (i) the TMA cation become trapped in the upper part of the cavity through cation- π interactions with the electron rich aromatic rings of the CTV moiety, and (ii) the anion is simultaneously bound in the lower part of the cage through hydrogen bonding with the amide functions. However, rather low binding constants (in the range of 10^2 M^{-1} , typically) were observed for the encapsulation of single anions, preventing reaching high binding constants in the presence of the cation. On the other hand, the remarkable affinity of urea groups for anions is well described.^[17] Aiming at increasing the affinity of hemicyptophanes for single anions, we present herein the design and synthesis of a novel heteroditopic cage **2**, which combines a CTV moiety and an amino-tris-urea unit (Figure 1). The positive effect of the incorporation of a urea motif in the hemicyptophane cage has been evaluated through the study of the encapsulation of six single anions. Furthermore, a remarkable positive cooperative effect has been demonstrated by the simultaneous binding of both anions and cations. Indeed, the hemicyptophane host **2** displays much better affinity for anions than our previously described hemicyptophane **1** and can recognize ion pairs with a strong positive cooperativity depending on the nature of the co-bound ions.



Scheme 1. Synthesis of hemicryptophane 2.

Results and Discussion

The synthetic pathway leading to the hemicryptophane **2** is shown in Scheme 1. Cyclotrimer derivative **3** is synthesized following a previously described two-step procedure: the reaction of 1,2-dibromoethane with vanillyl alcohol and subsequent cyclisation in the presence of scandium triflate in CH_3CN provide the CTV **3** in 11% yield.^[18] The CTV **4** is then obtained by mixing CTV **3** and *p*-hydroxybenzyl alcohol in DMF, using Cs_2CO_3 as a base. Compound **4** is then treated with sodium azide in the presence of triphenyl phosphine to give the intermediate **5** in 40% yield. Finally, the introduction of three isocyanate functions was achieved by bubbling CO_2 in a solution of **5** and triphenylphosphine; the subsequent reaction with the tren(tris-(2-aminoethyl)amine) under highly dilute conditions afforded hemicryptophane **2** in 13% yield.

The 1H NMR spectrum of hemicryptophane **2** in $CDCl_3$ shows, on average, C_3 symmetrical features (Figure 2). It displays the characteristic signals of the CTV unit: one singlet for the OMe group at 3.64 ppm, the AB system for the diastereotopic protons of the $ArCH_2$ bridges at 3.56 and 4.77 ppm, and two singlets for the aromatic protons at 7.03 and 6.83 ppm. The diastereotopic OCH_2CH_2O and $ArCH_2N$ methylene protons of the arms appear as multiplets between 3.6 and 4.5 ppm. The aromatic protons of the benzene ring of the linker give two doublets at 6.63 and 6.27 ppm. The signals of the urea and NCH_2CH_2N protons of the lower part of the cage appear as broad signals at 5.90 and 5.50 ppm, and 3.00 and 2.37 ppm, respectively.

The recognition of anions with host **2** was then investigated by 1H NMR titration experiments in $CDCl_3$. Tetra-*n*-butylammonium salts (TBA) ($nBu_4N^+X^-$) were used because the TBA cation is too big to enter inside the cavity of hemicryptophane cages.^[16] The host-guest exchange was found to be fast on the NMR timescale: only one set of signals was observed during the titration experiments, as usually reported with hem-

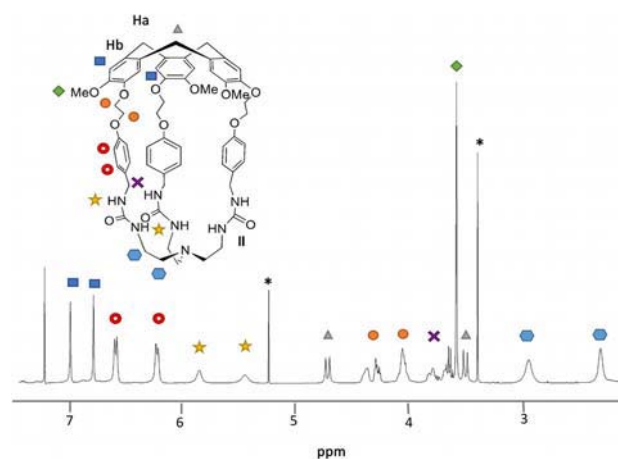


Figure 2. 1H NMR spectrum (400 MHz, $CDCl_3$) of **2**. *solvents (CH_2Cl_2 and CH_3OH).

cryptophane hosts. Upon progressive addition of a concentrated solution of the guest to a solution of **2** in $CDCl_3$, the NH protons exhibit a strong downfield shift, evidencing the presence of hydrogen-bonding interactions between these anions and the urea unit of **2** (Figures 3 a and S11–S16). Signals of the aromatic protons of the linkers also show significant shifts during these titration experiments. In contrast, the other protons of the host appear less affected. Altogether these observations are consistent with a complexation of the anion by the tris-urea moiety. The complexation-induced shifts of the H_a protons of the CTV unit have been chosen to be plotted as a function of the guest:host ratio because of their sharp and well-defined signals showing no overlapping with other peaks, whatever the anion added (Figures S11–S16). The resulting experimental titration curves were modeled using Bindfit program and the stoichiometry of host-guest complexes determined by fitting the titration curves using 1:1 or 1:2 host:guest

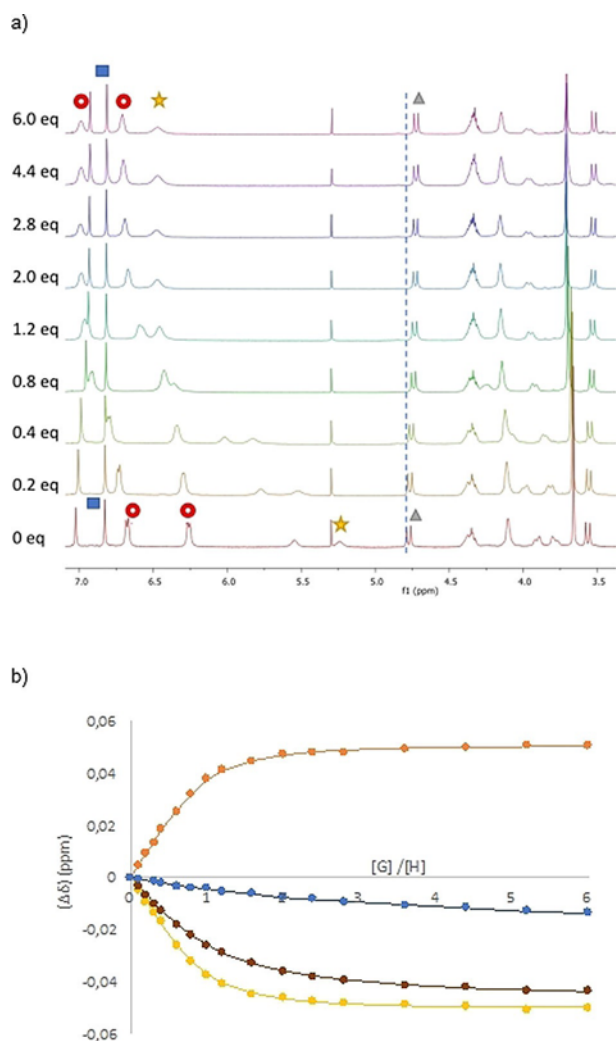


Figure 3. a) Example of the ^1H NMR monitoring of the titration of the host **2** (2.5 mM) with Cl^- (as a solution of TBACl salt, 25 mM) in CDCl_3 ; b) Titration curves of host **2** with TBA-halide salts in CDCl_3 (see Figure S17 for other anions). The chemical induced shifts $\Delta\delta$ of host's protons at 4.8 ppm were measured and plotted as a function of the ratio $[\text{G}]/[\text{H}]$ (dots). Curves were fitted with the Bindfit program (lines). Blue: I^- ; brown: Br^- ; Yellow: Cl^- ; orange: F^- (To avoid superposition, the titration curve of F^- is inverted ($-\Delta\delta$)).

ratios (Figures 3 b and S17).^[19,20] The 1:1 host:guest stoichiometry turns out to provide the best fit in all cases. The calculated binding constants are reported in Table 1. From these results, interesting features should be underlined. Firstly, the binding constants obtained with cage **2** are markedly higher than those previously measured with hemicyptophane **1**. For instance, the binding constants for Cl^- and H_2PO_4^- are increased by a factor 40 and 800 using **2**, respectively. Secondly, this binding constant improvement is associated with a remarkable increase of the selectivity. Contrary to host **1**, which poorly discriminates Cl^- from I^- , or H_2PO_4^- from AcO^- with 5:1 and 4:1 selectivity, respectively, host **2** turned out to be much more selective with ratios of 50:1 and 130:1 for the same anions. Thirdly, for spherical halide anions, the following affinity is observed: $\text{Cl}^- \approx \text{F}^- > \text{Br}^- > \text{I}^-$. This is in good agreement with the hydrogen-bond-accepting ability of this class of anions and

Table 1. Binding constants K_b (M^{-1}) for the 1:1 complexes formed between host **2** and anion guests.^[a]

Guest	K_b [M^{-1}], host 2	K_b [M^{-1}], host 1
F^-	3900	120
Cl^-	4100	100
Br^-	1050	65
I^-	80	20
AcO^-	1400	60
HSO_4^-	24800	45
H_2PO_4^-	184200	235

[a] K_b was determined by fitting ^1H NMR titration curves (CDCl_3 , 500 MHz, 300 K) on the Ha protons of the CTV unit (δ at 4.8 ppm for the free host) with the Bindfit program. More details on the calculations results (covariance and RMS) can be found in Table S1; estimated error 10%.

supports that hydrogen bonding events between the urea groups and the anions are responsible for this complexation. A better match between the size of the cavity and the one of the Cl^- anion could possibly account for the almost identical affinities observed for Cl^- and F^- . Fourthly, H_2PO_4^- displays a very high binding constant, probably because this tetrahedral anion can bind simultaneously with the six hydrogen atoms of the urea units.^[21] Hence, selectivities ranging from 1:8 to 1:2000, for I^- and HSO_4^- respectively, are reached.

Motivated by the improved affinity of **2** for single anions, we further investigate its ability to bind ion pairs. In a preliminary study we examined the binding of the tetramethylammonium-picrate (TMAPic) salt by hemicyptophane **2**. Due to its size, the picrate anion cannot access the cavity to interact with the NH functions of the host, therefore only the TMA cation can bind the CTV unit inside the cavity of **2**.^[16]

The ^1H NMR monitored titration studies reveals modification of the signals corresponding to the TMA guest, which appears upfield, confirming its complexation of TMA by through cation- π and CH- π interactions (Figure S18). However, upon progressive addition of host to a solution of the TMA guest, the signals corresponding to the guest appears significantly broadens preventing further titration curve drawing and binding constant determination. Nevertheless, this experiment evidences the interaction between this cation and host **2**. The ability of hemicyptophane **2** to simultaneously bind cations and anions was then studied. The $[\mathbf{2} \cdot \text{Me}_4\text{N}^+]$ complex was firstly prepared from the soluble $\text{Me}_4\text{N}^+\text{Pic}^-$ guest because of the lack solubility of the Me_4N^+ halide salts in chloroform (Figures S19–S21). Then, a solution of $n\text{Bu}_4\text{N}^+\text{X}^-$ was progressively added as source of halide anion guest. This allowed us to build a titration curve and determine the apparent binding constant (K_{app}) corresponding to the complexation of anions in the presence of a co-bound cation and thus to assess the cooperativity effect (see Figure S22 for the titration curves). Interestingly, the binding constants of anions are strongly improved by the presence of one equivalent of TMA ion inside the cavity, with K_{app} up to 29.10^3M^{-1} for the TMAcI ion pair (Figure 4). The additional electrostatic interaction between the anion and the cation already trapped inside the cavity can account for this positive cooperativity. The cooperativity factor

(K_{app}/K_a) is optimal for the Me_4NBr ion pair (around 13). Interestingly, the selectivity between F^- and Br^- is therefore inverted by the presence of the co-bound cation. This behavior could be explained by a closer match of the size and shape of the cavity of the cage by the Me_4NBr ion pair, allowing for (i) maximized cation- π interactions with the CTV unit, (ii) optimal hydrogen bonding of the anion with the tris-urea moiety, and (iii) a tight contact between the two ions. For the Me_4NF ion pair, the cooperativity factor is much less important, probably because the three previously mentioned interactions cannot be simultaneously optimized.

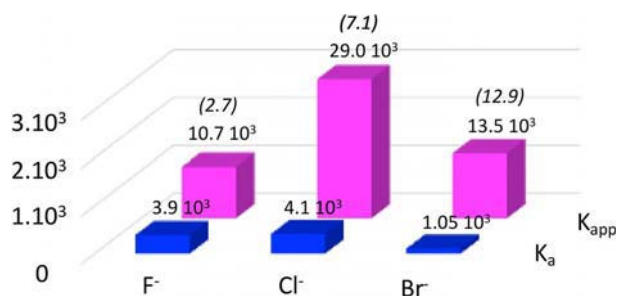


Figure 4. Comparison of binding constants for anions@**2** (K_a , blue) and anion@[$2\text{-Me}_4\text{N}^+$] (K_{app} , pink) complexes. Cooperativity factors are given in parentheses.

Further insight into this observed cooperativity was provided by analyzing the fully optimized geometry of ion-pair@hemicryptophane complexes obtained using DFT approach (Figure 5). In all cases hydrogen bonding can be observed between the anion guest and the urea units of the host: with $\text{N-H}\cdots\text{X}^-$ bound typically in the range of 1.8, 2.4 and 2.5 Å for F^- , Cl^- and Br^- respectively. Similarly, cation- π and $\text{CH}-\pi$ interactions are also evidenced in both cases with distances between some of the C-H of the ammonium guest and the aromatic rings of the CTV around 2.7 Å. Thus, host **2** can recognize both anions, through hydrogen bonding with its lower part, and cations, through cation- π interactions with its upper part, in agreement with the changes in chemical shift observed during the titration experiments. However, this kind of heteroditopic hosts must also be able to reconstitute the ion pair in the heart of their cavity. To examine this ability, we then compared the distance between the ions in the gas phase and in the cavity of hemicryptophane **2**. The change in the halide-nitrogen distance induced by the encapsulation shows that for

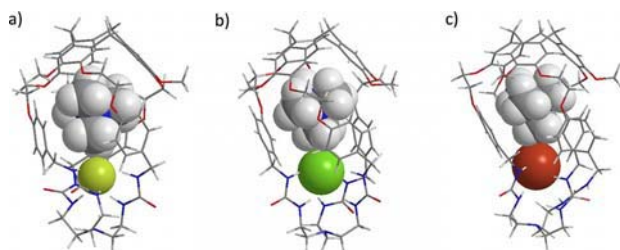


Figure 5. DFT-optimized structures of a) $2\text{-Me}_4\text{N}^+\text{F}^-$, b) $2\text{-Me}_4\text{N}^+\text{Cl}^-$, and c) $2\text{-Me}_4\text{N}^+\text{Br}^-$.

TMABr and TMACl, a lower increase in the ion pair separation is observed (The $\text{N}^+\cdots\text{X}^-$ distances are, respectively 33, 22 and 23% greater in the host than in gas phase for TMAF, TMACl and TMABr, respectively). Therefore, the coulombic interaction is negligibly disrupted with these two guests, which accounts for the enhanced observed cooperativity.

Conclusions

We have described the synthesis of a new hemicryptophane host **2** including a tris-urea unit. We demonstrate that the incorporation of the urea motif in the hemicryptophane structure is a promising strategy for the developments of highly efficient receptors able to simultaneously bind anions and cations with high binding constants. When compared with a previous similar structure, hemicryptophane **2** reveals markedly improved binding constants toward anions and selectivity. The heteroditopic character of this new host was further demonstrated through its ability to complex ion pairs with interesting positive cooperativity. The performed DFT calculations allow for a better understanding of the improved cooperativity factor observed for the Me_4NBr salt. Further investigations are in progress in our laboratory aiming at assessing the ability of hemicryptophane **2** to recognize zwitterions.

Experimental Section

Chemicals and materials. All chemicals were purchased from commercial sources and used without further purifications. All reactions were carried out under argon atmosphere and with anhydrous solvent (excepted CCl_4) purchased from commercial suppliers. THF was dried thanks to a solvent purification system (MB-SPS-800) under an argon flush. ^1H and ^{13}C NMR spectra were recorded in CDCl_3 on a Brüker Avance III (300 MHz and/or 400 MHz) and the residual solvent was used as internal standard. Chemical shifts (δ) are expressed in ppm and the coupling constant (J) are in Hz. Mass spectra (HRMS) were recorded by the mass spectrometry service at the Spectropole Aix Marseille Université. Melting points were determined with a Büchi Melting Point B-545. IR spectra were obtained using a Bruker Alpha Platinum ATR. Other compounds (CTV-Br) were synthesized according to literature procedure.^[18]

Synthesis of precursor triphenol 4. Hydroxybenzylalcohol (1.14 g, 9.2 mmol) and cesium carbonate (3.0 g, 9.2 mmol) were dissolved in DMF (40 mL). CTV-Br **3** (2.0 g, 2.7 mmol) was added and the mixture was heated at 40 °C for 3 days. Then, the reaction was cooled at room temperature and 100 mL of EtOAc and 100 mL of distilled water were added. The two layers were separated, and the aqueous phase was extracted with EtOAc (3×30 mL). The combined organic layers were washed with a solution of sodium hydroxide (10%) (3×30 mL) and NaCl saturated (50 mL), dried over Mg_2SO_4 and filtered. The solvent was removed under vacuum to give a white solid (1.76 g, 75%).

^1H NMR (CDCl_3 , 298 K, 400 MHz): $\delta = 7.24$ (d, $J = 8.7$ Hz, 2H, ArH), 6.95 (s, 1H, ArH), 6.86 (d, $J = 8.6$ Hz, 2H, ArH), 6.81 (s, 1H, ArH), 4.74 (d, $J = 13.7$ Hz, 1H, ArCH_2Ar), 4.60 (s, 2H, CH_2OH), 4.41–4.21 (m, 4H, OCH_2), 3.73 (s, 3H, OCH_3), 3.53 ppm (d, $J = 13.8$ Hz, 1H, ArCH_2Ar). ^{13}C NMR (CDCl_3 , 298 K, 101 MHz): $\delta = 158.34$ (C_{ar}), 148.88 (C_{ar}), 146.88 (C_{ar}), 133.71 (C_{ar}), 133.44 (C_{ar}), 132.06 (C_{ar}), 128.76 (C_{ar}H), 117.30 (C_{ar}H), 114.89 (C_{ar}H), 114.18 (C_{ar}H), 68.49 (OCH_2), 66.74 (OCH_2), 65.14 (CH_2OH), 56.37 (OCH_3), 36.62 ppm (ArCH_2Ar). ESI-MS

m/z : observed 876.3953 $[M+NH_4]^+$ (calculated: 876.3954 for $C_{51}H_{58}NO_{12}^+$). Mp: 228 °C. IR: $\tilde{\nu}$ =3368, 2921, 1508, 1247, 1214, 1142 cm^{-1} .

Synthesis of precursor triazide 5. To a solution of precursor triphenol **4** (524 mg, 0.61 mmol) dissolved in CCl_4/DMF (1/4) (20 mL) under argon atmosphere, were added triphenylphosphine (480 mg, 1.8 mmol) and sodium azide (142 mg, 2.2 mmol). The mixture was heated at 90 °C for 5 h then brought to room temperature and quenched by adding 10 mL of water. CH_2Cl_2 was added (30 mL) and the two layers were separated. The aqueous phase was extracted with CH_2Cl_2 (3×20 mL) and the organic solution was washed with water (3×20 mL) and NaCl saturated (50 mL), dried over $MgSO_4$, filtered and evaporated. The crude product was purified by column chromatography on silica gel using petroleum ether and ethyl acetate (1:4 then gradient to 1:1) to give a white solid (228 mg, 40%).

1H NMR ($CDCl_3$, 298 K, 400 MHz): δ =7.22 (d, J =8.5 Hz, 2H, ArH), 6.94 (d, J =8.4 Hz, 2H, ArH), 6.90 (s, 1H, ArH), 6.83 (s, 1H, ArH), 4.75 (d, J =13.8 Hz, 1H, $ArCH_2Ar$), 4.39–4.21 (m, 6H, $O(CH_2)_2O$ and $ArCH_2N_3$), 3.76 (s, 3H, OCH_3), 3.54 (d, J =14.0 Hz, 1H, $ArCH_2Ar$). ^{13}C NMR ($CDCl_3$, 298 K, 101 MHz): δ =129.71 ($C_{ar}H$), 117.24 ($C_{ar}H$), 114.97 ($C_{ar}H$), 114.21 ($C_{ar}H$), 68.42 (OCH_2), 66.65 (OCH_2), 56.27 (OCH_3), 54.36 (CH_2N_3), 36.47 ppm ($ArCH_2Ar$). ESI-MS m/z : observed 951.4149 $[M+NH_4]^+$ (calculated: 951.4148 for $C_{51}H_{55}N_{10}O_9^+$). Mp: 56 °C. IR: $\tilde{\nu}$ =2927, 2090, 1607, 1507, 1246, 1215, 1142 cm^{-1} .

Synthesis of hemicryptophane 2. Under argon atmosphere, precursor **5** (491 mg, 0.53 mmol) and triphenylphosphine (827 mg, 3.2 mmol) were dissolved in THF (20 mL). CO_2 was bubbled in the solution for 5 minutes and the reaction was stirred overnight under CO_2 atmosphere. Then, the CO_2 was replaced by argon and the reaction mixture was placed in a syringe. In another syringe was prepared, containing tris-2-aminoethyl amine (77.5 mg, 0.53 mmol) in THF (20 mL). The 2 syringes were added simultaneously dropwise in a 200 mL of THF. The reaction mixture was stirred for an hour and the solvent was removed under vacuum. The crude product was purified by column chromatography on silica gel using CH_2Cl_2 with a gradient of MeOH to give a white powder (77 mg, 13%).

1H NMR ($CDCl_3$, 298 K, 400 MHz): δ =7.03 (s, 1H, ArH), 6.83 (s, 1H, ArH), 6.63 (d, J =8.0 Hz, 2H, ArH), 6.27 (d, J =7.7 Hz, 2H, ArH), 5.90 (br, 1H, NH), 5.50 (br, 1H, NH), 4.77 (d, J =13.6 Hz, 1H, $ArCH_2Ar$), 4.36 (m, 2H, OCH_2), 4.11 (m, 2H, OCH_2), 3.91–3.67 (m, 2H, $ArCH_2NH$), 3.64 (s, 3H, OCH_3), 3.56 (d, J =13.8 Hz, 1H, $ArCH_2Ar$), 3.00 (br, 2H, $NH(CH_2)_2 N$), 2.37 ppm (br, 2H, $NH(CH_2)_2 N$). ^{13}C NMR ($CDCl_3$, 298 K, 101 MHz): δ =159.11 ($C=O$), 157.37 ($C_{ar}O$), 148.42 ($C_{ar}O$), 146.30 ($C_{ar}O$), 133.19 (C_{ar}), 131.86 (C_{ar}), 131.60 (C_{ar}), 128.27 ($C_{ar}H$), 117.06 ($C_{ar}H$), 114.63 ($C_{ar}H$), 113.56 ($C_{ar}H$), 67.77 (OCH_2), 67.68 (OCH_2), 55.81 (OCH_3), 54.98 ($NH(CH_2)_2 N$), 43.46 ($ArCH_2NH$), 38.64 ($NH(CH_2)_2 N$), 36.45 ppm ($ArCH_2Ar$). ESI-MS m/z : observed 1080.5086 $[M+NH_4]^+$ (calculated: 1080.5077 for $C_{60}H_{70}N_7O_{12}^+$). Mp: 116 °C. IR: $\tilde{\nu}$ =3306, 2949, 1658, 1630, 1508, 1254, 1221 cm^{-1} .

Titration experiments. A solution of host **2** (1.0 mM in $CDCl_3$, 500 μ L) was titrated in NMR tubes with aliquots of a concentrated solution (10 mM in the same solvent) of guests. The shifts $\Delta\delta$ of the host's protons signals at 6.90 ppm were measured after each addition and plotted as a function of the guest/host ratio ($[G]/[H]$). Association constant K_a was obtained by nonlinear least-squares fitting of these plots using Bindfit program from Thordarson's group.^[22] K_a , covariance and RMS are reported for each carbohydrate in the supporting information.

Computational method. All electronic structure calculations were carried out within density functional theory (DFT) framework. Since

the inspected systems are particularly flexible, intramolecular interactions are likely to dictate their shape. Therefore, weak interactions corrections were included by means of a nowadays current procedure. The energy contributions arising from atoms polarizabilities are added on top of the DFT electronic energy.^[23,24] Full geometry optimizations were performed using the B3LYP functional and 6-31G* a basis set in the Gaussian G09 suite of programs.^[25]

- [1] J. W. Steed, J. L. Atwood, *Supramolecular Chemistry*, Wiley, Chichester, 2009.
- [2] a) M. Ciardi, A. Galan, P. Ballester, *J. Am. Chem. Soc.* **2015**, *137*, 2047–2055; b) M. Ciardi, F. Tancini, G. Gil-Ramirez, E. C. E. Adan, C. Massera, E. Dalcanale, P. Ballester, *J. Am. Chem. Soc.* **2012**, *134*, 13121–13132; c) J. R. Romero, G. Aragay, P. Ballester, *Chem. Sci.* **2017**, *8*, 491–498; d) R. Molina-Muriel, G. Aragay, E. C. Escudero-Adán, P. Ballester, *J. Org. Chem.* **2018**, *83*, 13507–13514.
- [3] E. N. W. Howe, M. Bhadbhade, P. Thordarson, *J. Am. Chem. Soc.* **2014**, *136*, 7505–7516.
- [4] a) A. J. McConnell, P. D. Beer, *Angew. Chem. Int. Ed.* **2012**, *51*, 5052–5061; *Angew. Chem.* **2012**, *124*, 5138–5148; b) S. C. Picot, B. R. Mullaney, P. D. Beer, *Chem. Eur. J.* **2012**, *18*, 6230–6237.
- [5] a) S. K. Kim, J. L. Sessler, *Acc. Chem. Res.* **2014**, *47*, 2525–2536; b) S. K. Kim, V. M. Lynch, N. J. Young, B. P. Hay, C.-H. Lee, J. S. Kim, B. A. Moyer, J. L. Sessler, *J. Am. Chem. Soc.* **2012**, *134*, 20837–20843; c) Q. He, G. M. Peters, V. M. Lynch, J. L. Sessler, *Angew. Chem. Int. Ed.* **2017**, *56*, 13396–13400; *Angew. Chem.* **2017**, *129*, 13581–13585.
- [6] a) M. Cametti, M. Nissinen, A. D. Cort, L. Mandolini, K. Rissanen, *J. Am. Chem. Soc.* **2007**, *129*, 3641–3648; b) T. Mäkelä, K. Rissanen, *Dalton Trans.* **2016**, *45*, 6481–6490; c) T. Mäkelä, A. Kiesilä, E. Kalenius, K. Rissanen, *Chem. Eur. J.* **2016**, *22*, 14264–14272; d) M. Cametti, M. Nissinen, A. D. Cort, K. Rissanen, L. Mandolini, *Inorg. Chem.* **2006**, *45*, 6099–6101.
- [7] a) K. Ziach, M. Karbarz, J. Romański, *Dalton Trans.* **2016**, *45*, 11639–11643; b) S. Zdanowski, P. Piątek, J. Romański, *New J. Chem.* **2016**, *40*, 7190–7196; c) M. Karbarz, J. Romański, *Inorg. Chem.* **2016**, *55*, 3616–3623; d) R. Tepper, B. Schulze, P. Bellstedt, J. Heidler, H. Gork, M. Jäger, U. S. Schubert, *Chem. Commun.* **2017**, *53*, 2260–2263.
- [8] a) "Ion-Pair Recognition by Ditopic Macrocyclic Receptors": B. D. Smith in *Macrocyclic Chemistry: Current Trends and Future Perspectives* (Ed.: K. Gloe), Springer, Dordrecht, **2005**, pp. 137–151; b) J. M. Mahoney, K. A. Stucker, H. Jiang, I. Carmichael, N. R. Brinkmann, A. M. Beatty, B. C. Noll, B. D. Smith, *J. Am. Chem. Soc.* **2005**, *127*, 2922–2928; c) J. M. Mahoney, J. P. Davis, A. M. Beatty, B. D. Smith, *J. Org. Chem.* **2003**, *68*, 9819–9820.
- [9] A. Sengupta, Y. Liu, K. P. McDonald, M. Pink, J. R. Anderson, K. Raghavachari, A. H. Flood, *J. Am. Chem. Soc.* **2015**, *137*, 9746–9757.
- [10] K. Zhu, S. Li, F. Wang, F. Huang, *J. Org. Chem.* **2009**, *74*, 1322–1328.
- [11] a) S. K. Ray, A. Homberg, M. Vishes, C. Besnard, J. Lacour, *Chem. Eur. J.* **2018**, *24*, 2944–2951; b) M. Clemente-León, C. Pasquini, V. Hebbe-Viton, J. Lacour, A. D. Cort, A. Credi, *Eur. J. Org. Chem.* **2006**, 105–112.
- [12] M. Denis, L. Qin, P. Turner, K. Jolliffe, S. Goldup, *Angew. Chem. Int. Ed.* **2018**, *57*, 5315–5319; *Angew. Chem.* **2018**, *130*, 5413–5417.
- [13] a) S. K. Kim, J. L. Sessler, *Chem. Soc. Rev.* **2010**, *39*, 3784–3809; b) C. Caltagirone, P. A. Gale, *Chem. Soc. Rev.* **2009**, *38*, 520–563; c) J. M. Maho-

- ney, G. U. Nawaratna, A. M. Beatty, P. J. Duggan, B. D. Smith, *Inorg. Chem.* **2004**, *43*, 5902–5907; d) B. D. Smith, J. M. Mahoney in *Encyclopedia of Supramolecular Chemistry*, Vol. 2 (Eds.: J. L. Atwood, J. W. Steed), Pergamon, New York, **2004**, pp. 1291–1294; e) G. J. Kirkovits, J. A. Shriver, P. A. Gale, J. L. Sessler, *J. Inclusion Phenom. Macrocyclic Chem.* **2001**, *41*, 69–75; f) M. G. Antonisse, D. N. Reinhoudt, *Chem. Commun.* **1998**, 443–448; g) X. Wu, E. Howe, P. A. Gale, *Acc. Chem. Res.* **2018**, *51*, 1870–1879; h) H. Valkenier, A. P. Davis, *Acc. Chem. Res.* **2013**, *46*, 2898–2909.
- [14] T. Brotin, J.-P. Dutasta, *Chem. Rev.* **2009**, *109*, 88–130.
- [15] D. Zhang, A. Martinez, J.-P. Dutasta, *Chem. Rev.* **2017**, *117*, 4900–4942.
- [16] O. Perraud, V. Robert, A. Martinez, J.-P. Dutasta, *Chem. Eur. J.* **2011**, *17*, 4177.
- [17] a) P. A. Gale, N. Busschaert, C. J. E. Haynes, L. E. Karagiannidis, I. L. Kirby, *Chem. Soc. Rev.* **2014**, *43*, 205–241; b) P. Gale, J. T. Davis, R. Quesada, *Chem. Soc. Rev.* **2017**, *46*, 2497–2519; c) M. Rezanková, J. Budka, J. Miksátko, V. Eigner, I. Cisarová, P. Curinová, P. Lhoták, *Tetrahedron* **2017**, *73*, 742–749; d) O. Jurček, H. Valkenier, R. Puttreddy, M. Novák, H. A. Sparkes, R. Marek, K. Rissanen, A. P. Davis, *Chem. Eur. J.* **2018**, *24*, 8178; e) M. Olivari, R. Montis, L. E. Karagiannidis, P. N. Horton, L. K. Mapp, S. J. Coles, M. E. Light, P. A. Gale, C. Caltagirone, *Dalton Trans.* **2015**, *44*, 2138–2149; f) C. A. Offiler, C. D. Jones, J. W. Steed, *Chem. Commun.* **2017**, *53*, 2024–2027; g) N. Qureshi, D. S. Yufit, K. M. Steed, J. A. K. Howard, J. W. Steed, *CrystEngComm* **2016**, *18*, 5333–5337; h) C. M. Dias, H. Li, H. Valkenier, L. E. Karagiannidis, P. A. Gale, D. N. Sheppard, A. P. Davis, *Org. Biomol. Chem.* **2018**, *16*, 1083–1087; i) H. Li, H. Valkenier, L. W. Judd, P. R. Brotherhood, S. Hussain, J. A. Cooper, O. Jurček, H. A. Sparkes, D. N. Sheppard, A. P. Davis, *Nat. Chem.* **2016**, *8*, 24–32.
- [18] B. Chatelet, E. Payet, O. Perraud, P. Dimitrov-Raytchev, L.-C. Chapellet, V. Dufaud, A. Martinez, J.-P. Dutasta, *Org. Lett.* **2011**, *13*, 3706.
- [19] F. Ulatowski, K. Dąbrowa, T. Bałakier, J. Jurczak, *J. Org. Chem.* **2016**, *81*, 1746–1756.
- [20] URL: <http://app.supramolecular.org/bindfit/>.
- [21] V. B. Bregović, N. Basarić, K. Mlinarić-Majerski, *Coord. Chem. Rev.* **2015**, *295*, 80–124.
- [22] D. B. Hibbert, P. Thordarson, *Chem. Commun.* **2016**, *52*, 12792–12805.
- [23] S. Grimme, *Comput. Mol. Sci.* **2011**, *1*, 211.
- [24] S. Grimme, J. Antony, S. Ehrlich, S. Krieg, *J. Chem. Phys.* **2010**, *132*, 154104.
- [25] a) Gaussian 09 (Revision D.01), M. J. Frisch, G. W. Trucks, H. B. Schlegel, G. E. Scuseria, M. A. Robb, J. R. Cheeseman, G. Scalmani, V. Barone, B. Mennucci, G. A. Petersson, H. Nakatsuji, M. Caricato, X. Li, H. P. Hratchian, A. F. Izmaylov, J. Bloino, G. Zheng, J. L. Sonnenberg, M. Hada, M. Ehara, K. Toyota, R. Fukuda, J. Hasegawa, M. Ishida, T. Nakajima, Y. Honda, O. Kitao, H. Nakai, T. Vreven, J. A. Montgomery, Jr., J. E. Peralta, F. Ogliaro, M. Bearpark, J. J. Heyd, E. Brothers, K. N. Kudin, V. N. Staroverov, R. Kobayashi, J. Normand, K. Raghavachari, A. Rendell, J. C. Burant, S. S. Iyengar, J. Tomasi, M. Cossi, N. Rega, J. M. Millam, M. Klene, J. E. Knox, J. B. Cross, V. Bakken, C. Adamo, J. Jaramillo, R. Gomperts, R. E. Stratmann, O. Yazyev, A. J. Austin, R. Cammi, C. Pomelli, J. W. Ochterski, R. L. Martin, K. Morokuma, V. G. Zakrzewski, G. A. Voth, P. Salvador, J. J. Dannenberg, S. Dapprich, A. D. Daniels, O. Farkas, J. B. Foresman, J. V. Ortiz, J. Cioslowski, D. J. Fox, Gaussian, Inc., Wallingford CT, **2009**.